Journal of Communication Engineering (JCE)

P- ISSN: 2322-4088 Vol. 11, No. 2, Jul.-Dec. 2022 E- ISSN: 2322-3936

A Switchable Quadri-Polarized Dielectric Resonator Antenna

M. Rezvani* **[Corresponding Author]** 1Department of Civil Engineering; Cha.C.; IslamicAzad University; Chalous, Iran;
Email: masumerezvanii@gmail.com

S. Nikmehr Department of Electrical and Computer Engineering; University of Tabriz; Tabriz, Iran;
Email: nikmehr@tabrizu.ac.ir

A. Pourziad Department of Electrical and Computer Engineering; University of Tabriz; Tabriz, Iran;
Email: ali_pourziad@tabrizu.ac.ir

Received: *02 Jun. 2022* ***Revised:*** *23 Sep. 2022* ***Accepted:*** *10 Oct. 2022*

Abstract: In this work, a switchable quadri-polarized dielectric resonator antenna (DRA) is presented, capable of supporting four distinct polarization states: vertical linear polarization (VLP), horizontal linear polarization (HLP), left-handed circular polarization (LHCP), and right-handed circular polarization (RHCP). This feature enables the antenna to cater to polarization diversity, which is a critical requirement in modern wireless communication systems for enhancing signal reliability, reducing multipath fading, and improving overall system performance. The polarization switching mechanism is achieved using a simple yet effective microstrip feed line integrated with two pin diodes, which serve as control elements to dynamically reconfigure the antenna's polarization. This eliminates the need for complex feeding networks or mechanical rotation, making the design compact and easy to integrate into existing systems. The proposed DRA exhibits an impedance bandwidth of approximately 19.25%, a peak gain of about 7.73 dBi, and an axial ratio bandwidth close to 5%, ensuring efficient radiation performance across the operational band. These characteristics make it a promising candidate for applications such as 5G, IoT, and satellite communication systems.

Index Terms: Dielectric Resonator Antenna, Pin Diodes, Polarization Diversity.

Citation: M. Rezvani, S. Nikmehr, and A. Pourziad, "A Switchable Quadri-Polarized Dielectric Resonator Antenna," *Journal of Communication Engineering*, vol. 11, no. 2, pp. 281-294, Jul.-Dec. 2022.
http://dx.doi.org/10.22070/jce.2025.20450.1282

I. INTRODUCTION

Radio communication devices are becoming smaller and increasingly multifunctional. Concerning dimension restriction, coupling effect, the conventional solution of employing two or more antennas to realize multifunction or diversity schemes might be not achievable. Dielectric resonator antennas have been widely noticed due to their compact size, adjustable polarization, low loss in new communication systems [1-5].

The antennas with multi polarizations are widely used in the new wireless systems due to security, save power and cost [6-10]. To this end, some switching devices such as pin/varactor diodes, Micro-Electromechanical System (MEMS) and high-speed transistors are mixed into the communication devices [11-14].

So far, a few reconfigurable polarization antennas have been introduced in literature. A reconfigurable polarization antenna with circular polarization, including a semi-circular slot and two pin diodes has been introduced for 5G applications [15]. By changing the diodes states, a maximum gain of 4.8 dBi can be achieved using this antenna. Also, a square patch antenna to generate both linear and circular polarizations using a switchable slotted ground is introduced in [16]. As a complicated reconfigurable polarization antenna, a wideband antenna with four X-shape slots and four diodes is introduced in [17] to generate LHCP and RHCP polarizations. A wideband loop antenna with electronically switchable circular polarization with 7 dBi gain and 14.9% axial ratio bandwidth is investigated in [18].

In this work, a compact size dielectric resonator antenna with multi-polarizations, including two kinds of linear and circular polarizations is studied. To this end, two pin diodes are considered in the microstrip feed line to generate the desired polarization. In other words, the regarded switches have been used to connect and disconnect two orthogonal microstrip lines. In OFF state, the DRA generates radiation eave with vertical and horizontal polarizations. In ON state, the DRA can be used to propagate LHCP and RHCP waves. The reflection coefficient of the antenna remains at the same level in ON or OFF state modes. Additionally, the most important parameters are changed to find the best performance of the antenna.

The cylindrical DRA supports resonant modes, particularly the TM_{110} mode, which has a simple and predictable field distribution. This makes it easier to design for dual orthogonal modes necessary for circular polarization. Its cylindrical symmetry ensures an omnidirectional, broadside radiation pattern and facilitates achieving equal amplitude orthogonal fields. Cylindrical DRAs are compact, efficient, and can support two orthogonal degenerate modes that can be excited independently or simultaneously. Using two orthogonal feed lines and PIN diodes, these modes can switch between various polarizations, including vertical, horizontal, and circular (both left

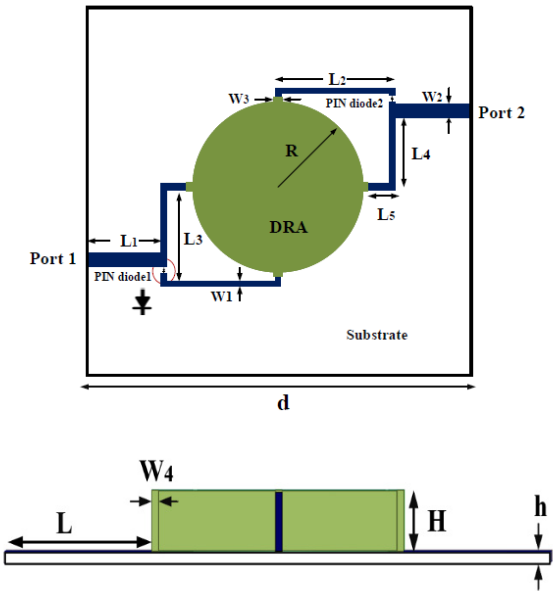

Fig. 1. Configuration of the proposed antenna (a) top view, (b) side view

and right-handed). Additionally, cylindrical DRAs have low conductor loss since they don't require metal cavity walls.

In the next section, first, closed-form expression formulas are introduced to estimate the initial dimensions of the antenna. In the following, the simulated results via HFSS software are reported. The results of the parametric study of the antenna are also shown. The last section summarizes the work.

II. ANTENNA DESIGN

The configuration of the proposed antenna is illustrated in Fig. 1. We used a two-step approach to determine the antenna dimensions, combining analytical formulas and full-wave simulation optimization. We start from closed-form expressions for the cylindrical DRA resonant frequency. As shown in Fig. 1, the designed reconfigurable polarization dielectric resonator antenna is formed of a cylindrical-shaped dielectric resonator antenna (DRA) with four vertical cubes, a feed structure, two pin diodes and a ground plane. In addition, four vertical PEC strips with the same heights are utilized in the antenna which is fed by a microstrip line mechanism.

The resonant frequency of the fundamental mode (TM_{110}) of a cylindrical-shaped DRA, which has the lowest resonant frequency can be calculated as [19]:

$$f_{TM\,110} = \frac{1}{2\pi R\sqrt{\mu\varepsilon}}\sqrt{3.39+\left(\frac{\pi R}{2H}\right)^2} \tag{1}$$

where μ, ε, H and R are the magnetic permeability, electric permittivity, height and radius of

the cylindrical-shaped DRA, respectively. This equation is not accurate. In [20], an empirical formula with acceptable accuracy is proposed to estimate the sizes of cylindrical-shaped DRA for a specified resonant frequency at the fundamental mode.

$$f_{res} = \frac{3.16c_0}{\pi R\sqrt{\varepsilon_{eff}+2}}\left[0.27+0.36\frac{R}{2h_{eff}}+0.02\left(\frac{R}{2h_{eff}}\right)^2\right] \quad (2)$$

where c_0 is the wave velocity of vacuum. Also, ε_{eff} and h_{eff} are the effective permittivity and the total height of the whole DRA, respectively. In Eq. (2) effective permittivity should be used. The resonant frequency depends on where the fields exist. Part of the fields are in the DRA, and part are in the surrounding substrate/air. Therefore, an effective permittivity is used to approximate the combined effect. These parameters are found as follows:

$$\varepsilon_{eff} = \frac{h_{eff}}{\frac{H}{\varepsilon_{DRA}}+\frac{h}{\varepsilon_{sub}}} \quad (3)$$

$$h_{eff} = H + h \quad (4)$$

where ε_{DRA} and ε_{sub} are the dielectric permittivity of DRA and substrate, respectively. A conventional cylindrical-shaped DRA has a linear polarization. To have a circularly polarized DRA, two orthogonal components of electric/magnetic fields in phase quadrature must be excited. To this end, two double branch microstrip feeds are considered to generate two orthogonal components. The phase difference ($\Delta\varphi$) between two branches is calculated as:

$$\Delta\varphi = \frac{2\pi}{\lambda}\Delta L \quad (5)$$

where ΔL is the patch difference and λ shows the wavelength. According to the DRA theory for a cylindrical-shaped DRA, the equivalent magnetic currents components on the side, top, and bottom walls can be analytically determined as follows [19]:

$$M_{\text{side wall}} = \frac{0.291\pi}{j\,\omega\varepsilon RH}\sin\varphi'\sin\frac{\pi z'}{2H}\hat{z} + \frac{1.972}{j\,\omega\varepsilon R^2}\cos\varphi'\cos\frac{\pi z'}{2H}\hat{\varphi} \quad (6)$$

$$M_{\text{tope/up wall}} = \frac{1.841\pi}{j\,2\omega\varepsilon RH}J_1'\left(\frac{1.841\rho'}{R}\right)\cos\varphi'\hat{\varphi} + \frac{\pi}{j\,2\omega\varepsilon H\,\rho'}J_1'\left(\frac{1.841\rho'}{R}\right)\sin\varphi'\hat{\rho} \quad (7)$$

In above equations $J_1(.)$ is the Bessel function of the first kind.

Since the radiation power are typically expressed in spherical coordinates, the equivalent magnetic currents components should be transformed as follows [21]:

$$M_\theta = M_\rho\cos\theta\cos(\varphi-\varphi') + M_\varphi\cos\theta\sin(\varphi-\varphi') - M_z\sin\theta \quad (8)$$

$$M_{\varphi} = -M_{\rho}\sin\left(\varphi-\varphi'\right)+M_{\varphi}\cos\left(\varphi-\varphi'\right) \tag{9}$$

By calculating the electric vector potentials (F_{θ}, $F\varphi$) using the following equations, the far-field components of the electric fields E_{θ}, $E\varphi$ are easily determined:

$$F_{\theta} = \frac{e^{-jk_0 r}}{4\pi r}\iiint M_{\theta} G\left(\rho',\varphi',z'\right)\rho' d\,\rho' d\,\varphi' dz' \tag{10}$$

$$F_{\varphi} = \frac{e^{-jk_0 r}}{4\pi r}\iiint M_{\varphi} G\left(\rho',\varphi',z'\right)\rho' d\,\rho' d\,\varphi' dz' \tag{11}$$

where,

$$G\left(\rho',\varphi',z'\right) = \mathrm{e}^{jk_0\left[\rho'\sin\theta\cos(\varphi-\varphi')+z'\cos\theta\right]} \tag{12}$$

In summary, equations 6 to 9 mathematically formalize how the DRA's geometry and feed mechanism generate the necessary field components for CP. The Bessel functions and trigonometric terms in Equations 6 to 7 describe the spatial distribution of fields, while Equations 8 to 9 link these to measurable far-field patterns.

By adjusting the location of feeds and length of them, two orthogonal components and corresponding circular polarization can be easily achieved. It should be noted that the proposed formulas are used to guess the initial calculations. The value of final parameters should be evaluated using the software facilities.

The proposed DRA using a ceramic compound with relative permittivity of 9.8 is etched on a 100×100×1.524 mm^3 Rogers RO4003 with dielectric constant of 3.55 and a loss tangent of 0.0027.

The main advantage of the proposed structure is that by switching ON or OFF the pin diodes (SMP1320 011F) which are modeled via a lumped element network [14], the linear or circular polarization is achieved. When a suitable voltage V_{p} is applied, the pin diode is forward-biased, connects two orthogonal microstrip feed lines and creates a 90-degree phase shift in ON state. In OFF mode, the diode is reverse biased. The dimensions of the proposed DR antenna are listed in Table 1.

It should be noted that the effects of the bias network and DC isolation circuits are not explicitly modeled in the performance evaluation. In the simulations, the PIN diodes are represented by equivalent lumped RLC circuits, rather than including a full biasing network. The initial concept and performance are demonstrated without modeling the DC bias network, to isolate the electromagnetic behavior of the antenna.

Table 1. Physical parameters of the proposed reconfigurable polarization antenna

Parameter	Value (mm)	Parameter	Value (mm)
L_1	20	W_1	0.9
L_2	28.65	W_2	3.6
L_3	23.55	W_3	0.9
L_4	18.05	W_4	1.17
L_5	6.83	R	22
L	26.83	H	9.1
d	100	h	1.524

III. RESULTS AND DISCUSSION

In this section, the performance of the proposed DR antenna in terms of reflection coefficient, antenna gain and axial ratio bandwidth is investigated in all switch states (Table 2) using HFSS, and CST simulator. Fig. (2) shows the s-parameters of the proposed DR. This antenna has a wide impedance bandwidth of 19.25% around the resonant frequency 4 GHz.

When one of the two diodes is in ON mode, all vertical stripes on the dielectric antenna surface are connected to the microstrip feed and circular polarization is obtained. In this case, two orthogonal strips generate two orthogonal modes with equal magnitude and 90-degree phase shift. The electric field distribution inside the dielectric resonator antenna has been illustrated in Fig. 3 at resonant frequency for different values of phases 0^o, 90^o, 180^o, and 270^o. Also, Fig. (4) shows the field distribution of DRA in OFF mode. In this case, the DRA has a linear polarization. Fig. 5 compares the axial ratio of the antenna for linear and circular polarization. For the circular polarization, the 3dB axial ratio bandwidth of the DRA is around 5%. When two switches are in OFF mode, the generated far-field patterns are linearly polarized. Therefore, by changing the Pin diodes status, the LHCP, RHCP, LP-V (vertical), and LP-H (Horizontal) polarizations can be achieved. The radiation pattern of the designed DR for the different cases is shown in Fig. 6. In addition, as shown in Fig. 7, the proposed antenna attains the peak gain of 7.73dB across the axial ratio bandwidth.

In order to improve the axial ratio bandwidth in circular polarization, several parametric studies are carried out. These studies incorporate the height of the vertical PEC strip, the height of the DRA and the width of the vertical DRA. Fig. 8 and Fig. 9 indicate the curves of the return loss and axial ratio variation with different values of *h* when one of the two switches is in ON state. As shown in Fig. 8, by increasing the height of the vertical strips, resonance frequency moves to higher frequencies and the impedance bandwidth increases. It can be observed in Fig. 9 that

Table 2. Different Pin Diode's States

		Port #1		Port #2	
Diode #1	On	LHCP		-	-
	Off	LP-V		-	-
Diode #2	On	-	-	RHCP	
	Off	-	-	LP-H	

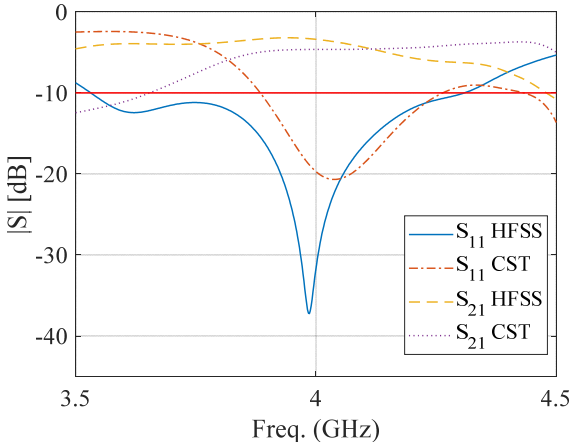

Fig. 2. S-parameters of the proposed antenna

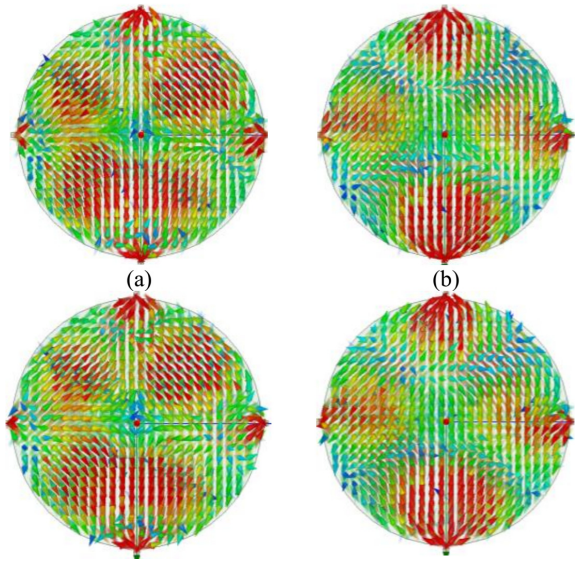

Fig. 3. E-field distribution inside the DRA at resonance frequency when one of the two switches are ON: (a) E-field, phase 0; (b) E-field, phase 90; (c) E-field, phase 180; (d) E-field, phase 270 (Circular polarization)

by decreasing the value of h, the axial ratio bandwidth decreases. As a result, for h=9mm, both impedance and axial ratio bandwidth are simultaneously improved.

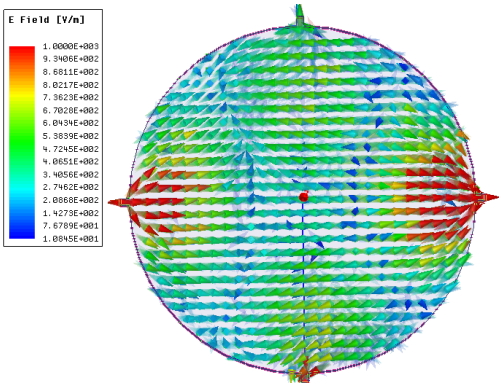

Fig. 4. E-field distribution inside the DRA at resonance frequency when two switches are OFF (Linear polarization)

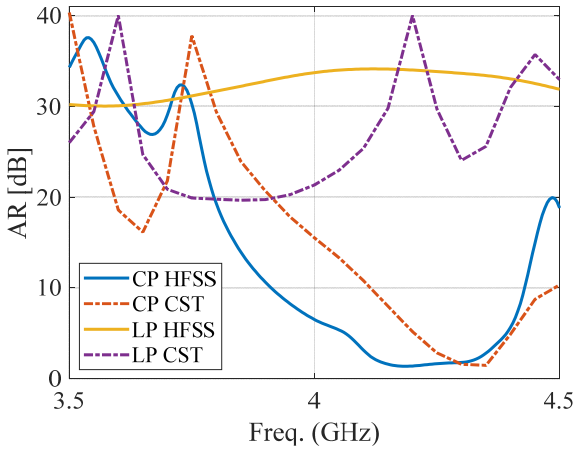

Fig. 5. The axial ratio of the proposed antenna

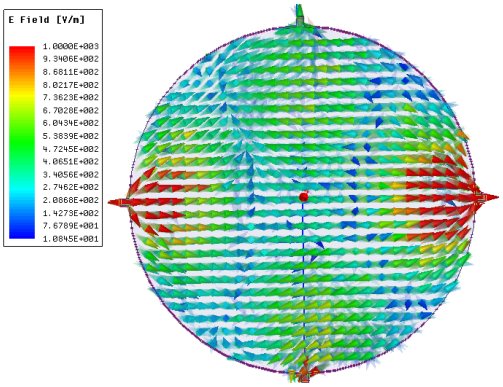

Fig. 6. Radiation pattern of the antenna at (a) 4GHz when diode#1 or diode #2 is ON (b) 4GHz (diode#1: ON and diode#2: OFF)/ (diode#1: OFF and diode#2: ON)

Fig. 10 and Fig. 11 illustrate the variations of the reflection coefficient and axial ratio versus the height of DR in ON mode. As depicted in Fig. 10, by changing the value of *H* from 9.1mm to 10mm, the resonance frequency and impedance bandwidth shift up from 3.95GHz to 3.98GHz and 400MHz to 770MHz, respectively. Also, it can be seen in Fig. 11 that when the DRA height

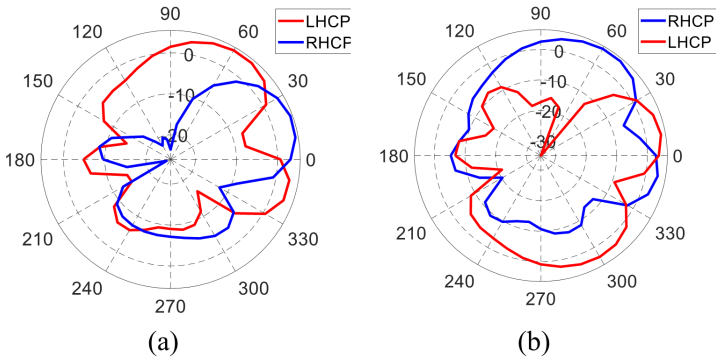

Fig. 7. The total gain of the proposed antenna

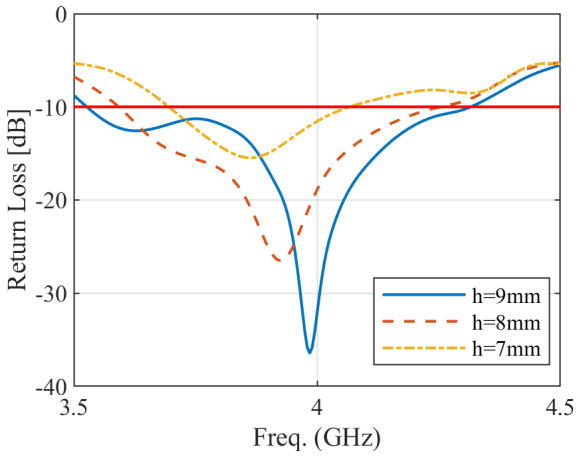

Fig. 8. The effect of various substrate thickness on the return loss

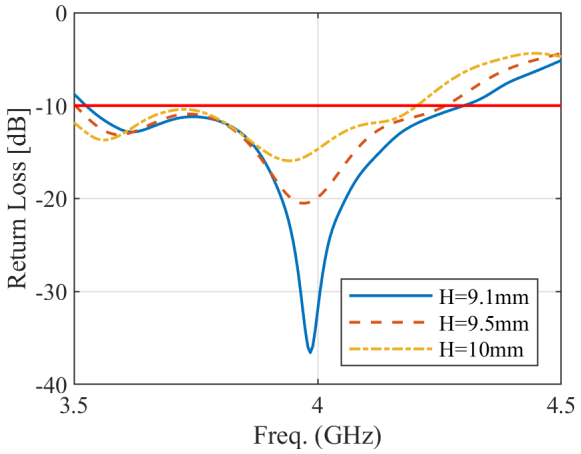

Fig. 9. The effect of various substrate thickness on the axial ratio

decreases, the axial ratio bandwidth increases.

Further reducing *H* below 9 mm might not necessarily yield better results. Fig. 11 suggests that a shorter DRA enhances the phase quadrature between orthogonal modes, which is essential for CP. Fig. 10 shows that reducing *H* shifts the resonant frequency upward and alters the impedance

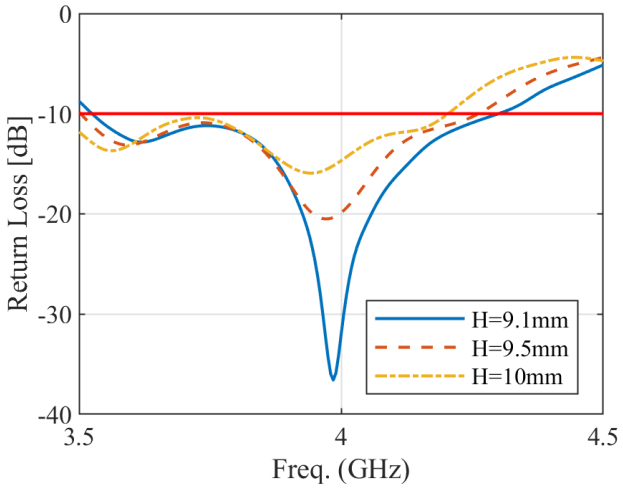

Fig. 10. The effect of various height of the DRA on the return loss

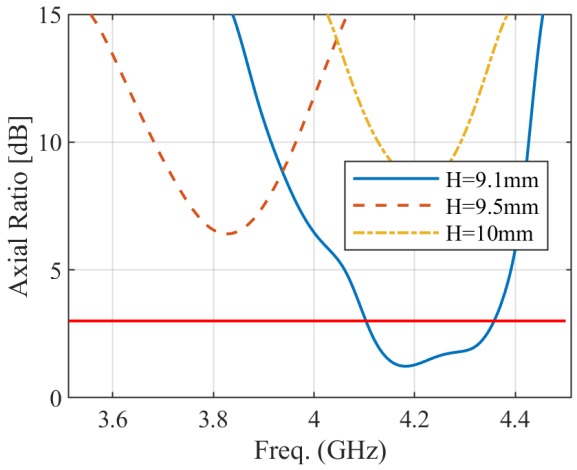

Fig. 11. The effect of various height of the DRA on the axial ratio

bandwidth. If H is too small, the antenna might struggle to maintain a good reflection coefficient, leading to poor power transfer. A shorter DRA reduces the effective radiating volume, potentially lowering antenna gain. Extremely small H could make the DRA difficult to manufacture or mechanically fragile. While smaller H improves AR bandwidth, it may narrow the impedance bandwidth (Fig. 10). The TM_{110} mode (used here) depends on H for proper field distribution. If H is too small, higher-order modes may dominate, degrading CP purity.

The variation of the return loss and axial ratio of the proposed antenna versus different values of the dielectric stub thickness (W_4=W) are shown in Fig. 12 and Fig. 13, respectively. By increasing the value of W up to 1.5mm, the impedance bandwidth decreases and the resonance frequency move to upper frequencies. Additionally, increasing the value of W, changes the antenna polarization from CP to LP. As a result, performance of the antenna is acceptable for h=9mm, H=9.1mm, and W=0.9mm in ON mode.

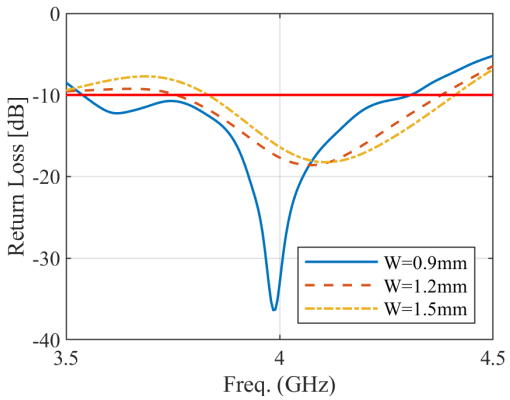

Fig. 12. The effect of various W on the return loss

Table 3 compares the performance of the proposed antenna with other works in terms of gain (G), Impedance Bandwidth (IB) and Axial Ratio Bandwidth (ARB). This comparison shows that the proposed DRA has higher peak gain, wider axial ratio bandwidth. Also, four kinds of polarization, including VLP, HLP, LHCP, and RHCP can be achieved using the DRA. Additionally, the proposed DRA has a lower number of pin diodes.

The paper highlights several advantages and innovations of the proposed antenna design. Unlike previous designs that offer dual or triple polarization, this antenna achieves all four polarizations (LP, LHCP, RHCP, and one more) using only two diodes, offering a simpler and more compact solution. The design eliminates the need for complex feed networks, branch-line couplers, or mechanical rotation, which reduces both fabrication costs and size. The antenna provides higher gain, a wider axial ratio bandwidth, and requires fewer switching elements compared to previous designs, resulting in improved performance. The use of a cylindrical dielectric resonator (DRA) ensures low conduction loss, compact size, and is ideal for polarization diversity due to its degenerate orthogonal modes, making it a low-loss, compact design.

IV. CONCLUSION

In this research work, a low-profile dielectric resonator antenna with four different polarizations is introduced. The proposed antenna can be used to generate the electromagnetic wave with both vertical and horizontal linear polarizations, and also left-handed and right-handed circular polarizations. To this end, two pin diodes are employed to switch the polarization between linear and circular one. Also, the effect of the most important geometrical parameters on the antenna performance has been studied. The gain, impedance bandwidth, and axial ratio bandwidth of the proposed DRA are around 7.73 dBi, 19.25% and 5%, respectively. Hence, this antenna is a good candidate for the polarization diversity applications for the modern radiocommunication systems.

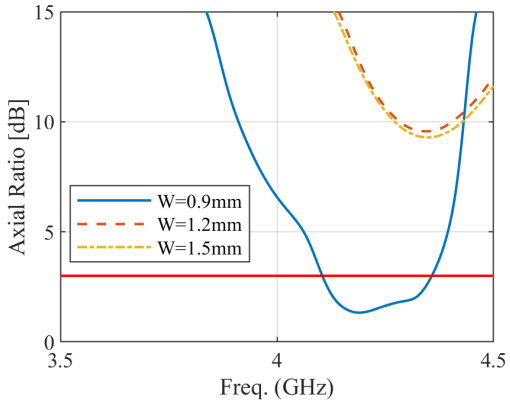

Fig. 13. The effect of various *W* on the axial ratio.

Table 3. Comparison Between The Proposed Antenna and Other Existing Structures

Ref.	IB	No. of switches	G	ARB	Polarization states
[16]	79MHz	8	7.1dBi	79MHz	LP-LHCP RHCP
[22]	250MHz	4	6.2dB	62.5MHz	LP-LHCP RHCP
[23]	1.36GHz	2	2.7dBi	90-220-90MHz	LHCP RHCP
This work	770MHz	2	7.73dB	200MHz	LP-V, LP-H, LHCP-RHCP

REFERENCES

[1] A. Dastranj, S. Heidari, "A 2-60 GHz Microwave and Millimeter-Wave Planar Antenna with Simple Structure," *Journal of Communication Engineering*, vol. 0, p. 305-317, June 2024

[2] A. Dastranj, Z. Javidi, "A Miniaturized Fractal Defected Ground Structure Super-Widedband Antenna for Wireless Communication Systems," *Journal of Communication Engineering*, vol. 10, p. 305-317, July 2021

[3] Z. Rahimian, S. Nikmehr, A. Pourziad, "A Novel Circularly polarized dielectric resonator antenna with Branch-Line Coupler and Log-Periodic Balun," *Journal of Communication Engineering*, vol. 7, p. 11-22, June 2018

[4] S. Yu, C. K. Wang, Y. M. Pan and S. Y. Zheng, "A Compact Singly Fed Dielectric Resonator Antenna with Flat-Top Radiation Patterns," *IEEE Trans. Antennas and Propagation*, vol. 72, no. 3, pp. 2096-2107, March 2024.

[5] M. M. Sani, R. Chowdhury and R. K. Chaudhary, "An Ultra-Wideband Rectangular Dielectric Resonator Antenna with MIMO Configuration," *IEEE Access*, vol. 8, pp. 139658-139669, July 2020

[6] W. Lin, et. al., "Circularly polarized antenna with reconfigurable broadside and conical beams facilitated by a mode switchable feed network," *IEEE Trans. Antennas and Propagation*, vol. 66, no. 2, pp. 996-1001, Feb. 2017.

[7] J. Hu, & Z. C. Hao, "A compact polarization-reconfigurable and 2-D beam-switchable antenna using the spatial phase shift technique," *IEEE Trans. Antennas and Propagation*, vol. 66, no. 10, pp. 4986-4995, Oct. 2018

[8] Y. I. Abdulraheem, et. al., "Design of frequency reconfigurable multiband compact antenna using two PIN diodes for WLAN/WiMAX applications," *IET Microwaves, Antennas & Propagation*, vol. 11, no. 8, pp. 1098-1105, May 2017.

[9] Y. Wang, "Design and investigation of differential-fed ultra-wideband patch antenna with polarization diversity," *International Journal of Antennas and Propagation*, November 2016.

[10] W. Lin, "Reconfigurable, wideband, low-profile, circularly polarized antenna and array enabled by an artificial magnetic conductor ground," *IEEE Transactions on Antennas and Propagation*, vol. 66, no. 3, pp. 1564-1569, March 2018.

[11] P. Kumar, S. Dwari, R. K. Saini, & M. K. Mandal, "Dual-band dual-sense polarization reconfigurable circularly polarized antenna," *IEEE Antennas and Wireless Propagation Letters*, vol. 18, no. 1, pp. 64-68, Jan. 2018.

[12] Y. Sung, "Investigation into the polarization of asymmetrical-feed triangular microstrip antennas and its application to reconfigurable antennas," *IEEE Trans. Antennas and Propagation*, vol. 58, no. 4, pp. 1039-1046, April 2009.

[13] B. Kim, "A novel single-feed circular microstrip antenna with reconfigurable polarization capability," *IEEE Trans. Antennas and Propagation,* vol. 56, no. 3, pp. 630-638, March 2008.

[14] Z. Yang, "Bandwidth enhancement of a polarization-reconfigurable patch antenna with stair-slots on the ground," *IEEE Antennas and Wireless Propagation Letters*, vol. 13, pp. 579-582, March 2014.

[15] Y. I. Al-Yasir, "A new polarization-reconfigurable antenna for 5G applications," *Electronics*, vol. 7, no.11, Nov. 2018.

[16] R. K., Saraswat, M. Kumar, S. Gurjar, & C. P. Singh, "A Reconfigurable Polarized Antenna Using Switchable Slotted Ground Structure," *In 2015 Fifth International Conference on Communication Systems and Network Technologies*, pp. 15-19, April 2015.

[17] Z. Mahlaoui, et. al., "Design of a Dual-Band Frequency Reconfigurable Patch Antenna Based on Characteristic Modes," *International Journal of Antennas and Propagation*, vol. 2019, pp. 1-12, March 2019.

[18] L. Zhang, et. al., "Wideband loop antenna with electronically switchable circular polarization," *IEEE Antennas and Wireless Propagation Letters*, vol. 16, pp. 242-245, May 2016.

[19] A. Petosa, Dielectric Resonator Antenna Handbook, Artech, 2007.

[20] R. Chowdhury, N. Mishra, M. M. Sani and R. K. Chaudhary, "Analysis of a Wideband Circularly Polarized Cylindrical Dielectric Resonator Antenna with Broadside Radiation Coupled with Simple Microstrip Feeding," *IEEE Access*, vol. 5, pp. 19478-19485, Sept. 2017.

[21] C. A. Balanis, Antenna Theory: Analysis and Design, John Wiley & Sons, 2016.

[22] F. Farzami, S. Khaledian, B. Smida, & D. Erricolo, "Reconfigurable linear/circular polarization rectangular waveguide filtenna," *IEEE Trans. Antennas and Propagation*, vol. 66, no. 1, pp. 9-15, Jan. 2017.

[23] T. T. Le, "Simple Reconfigurable Circularly Polarized Antenna at Three Bands," *Sensors*, vol. 19, no. 10, May 2019.

Journal of Communication Engineering (JCE)